Modelling chalcopyrite combustion together with fluid flow simulation

Tapio Ahokainen[1], Ari Jokilaakso[2], Jussi Vaarno[1], Juha Järvi[1]

1. Laboratory of Materials Processing, Helsinki University of Technology, Espoo, Finland
2. Academy of Finland

ABSTRACT

A mathematical model for chalcopyrite combustion in the flash smelting furnace reaction shaft is presented. Particle oxidation kinetics is modelled with a shrinking core model. The effect of mass transfer modes on the particle temperature and mineral composition during separate steps of the reaction is examined in laminar-flow conditions. It is found that during the reactions the controlling mode of mass transfer is shifted from thermally induced decomposition to pore diffusion and further to external bulk diffusion. Calculated maximum particle temperatures and sulphur removal are compared to published experimental data from laminar-flow studies. The kinetic module is combined with a commercial fluid flow solver and examples of the results of the flow and heat transfer simulation together with chalcopyrite combustion in an industrial scale flash smelter are presented.

1. INTRODUCTION

The flash smelting process (Bryk et al., 1958) and particularly the flash smelting furnace is an essential part of modern copper making practice. It utilises the heat of oxidation of sulphidic concentrate. Chalcopyrite is a traditional input material, but composition of the feed may vary depending on the origin of the ore. The feed mixture in the flash smelting process (concentrates, flux, reverts, and the process gas) is fed through the concentrate burner into the reaction shaft. Then, the concentrate particles react vigorously with oxygen in the gas phase leading to several phase changes and finally to melting of the particle. After the reaction shaft, the particle-gas suspension flows to the settler, where the particles/drops separate from the gas and form slag and matte layers. The gases continue to the uptake, through which they flow to a waste-heat boiler.

After ignition, chalcopyrite particles in the gas-particle suspension are at a much higher temperature than the gas stream, and inevitably heat transfer take place from particles to the gas phase. Typically particles are small (< 36 μm) and convection is the dominant heat transfer mode due to a large particle specific surface area and radiation interacts mainly between the reactor wall and gas-solid suspension. During heterogeneous chemical reactions, mass transfer of chemically reacting gas species plays an important role. Such phenomena as pore diffusion, and gas- and liquid-phase diffusion are characteristic to the system. To describe all this mathematically requires plenty of experimental knowledge about the process as well as efficient tools to solve the multiphase fluid flow coupled with heat/mass transfer.

One of the few pioneers of mathematical modelling of metallurgical processes was Ruottu who simulated the Outokumpu flash smelting process in the 1970s (Ruottu, 1979). That study was not continued, however, perhaps because the time had not yet come for modelling. During the 1980s Themelis et al. (Jiao et al., 1986; Kim, 1986) and Sohn and his group (Hahn&Sohn, 1987; 1990) made valuable modelling efforts in this field. At that time the models of the flash smelting furnace were one- or two-dimensional and the geometry of the concentrate burner was greatly simplified. On the other hand, the chemical reactions and heat transfer were already fairly comprehensively included. Both groups used their own codes for fluid flow, heat transfer, and turbulence, which is most probably a result of the early stage of commercially available packages at that time.

More recently, two research groups have adopted a commercial package for simulation of the flash smelting process in a more detailed way: Jorgensen and co-workers (Smith, 1991; Jorgensen&Elliot, 1992; Nguyen et al., 1992; Jorgensen et al., 1995) are concentrating on modelling the nickel flash smelting operations in the Kalgoorlie smelter of Western Mining Corporation, Australia; Jokilaakso and his group (Jokilaakso et al., 1994; Ahokainen&Jokilaakso, 1996) are dealing with the copper flash smelting process of Outokumpu, Finland.

In this paper, a mathematical model for chalcopyrite particle combustion is presented. The model includes the oxidation scheme proposed by Kim (Kim, 1986) for simulating gas-particle reactions in a flash smelting furnace. The kinetics and thermodynamics of the oxidation reactions are written as a separate module and then connected to the calculation of the flow field which, together with particle trajectories in the flow field, is solved by a commercial fluid flow package, Phoenics. The kinetic module and its connection to fluid flow and heat transfer calculation is still under development, and further testing and validation of the program is continuing. Anyway, a huge amount of preliminary results about the concentrate combustion in a two-dimensional calculation grid of an industrial scale flash smelting furnace have been obtained. Some of these results are presented in this paper.

2. NOMENCLATURE

A area (m^2)
d diameter (m)
D diffusivity (m^2/s)
h heat transfer coefficient (W/m^2K)
H enthalpy (J/kgO_2)
k rate coefficient (m/s)
k_d mass transfer coefficient (m/s) $= Sh D_{O_2}/d_p$
L liquid film thickness (m)
m mass (kg)
N number
$\dot{q}$ heat flux (W/m^2)
$\dot{Q}$ heat (W)
S source term
t time (s)
T temperature (K)
u velocity (m/s)
Y mass fraction
x co-ordinate direction

Greek letters

α absorptivity
α mass of sulphur divided by mass of chalcopyrite in particle at time = 0, eq.(16)
ε emissivity
ε' effective emissivity
Γ Exchange coefficient
ϕ General flow variable
η particle number density (1/s)
λ Thermal conductivity (W/mK)
ρ density (kg/m^3)
σ Stefan-Boltzmann constant $=5{,}67\cdot10^{-8}$ W/m^2K^4
τ' thermal time constant (s), $=\rho_p d_p^2 C_{p,p}/6\mathrm{Nu}\lambda_g$

Subscripts

c convection
c1 first shrinking core (original sulphide)
c2 second shrinking core (thermally decomposed sulphide)
dis dissociation reaction with sulphur oxidation
eff effective
g gas phase
h enthalpy
l liquid
n summation index
ov overall
ox oxidation reactions
p particle
r radiation
r reaction (eq. 4)
s due to chemical reactions
S sulphur
WRL within reacted layer

Superscripts

0 old value
p particle

3. NUMERICAL MODELLING METHOD

3.1 Gas-phase equations

The numerical simulation of the flash smelting process was carried out with Phoenics, which is a general-purpose solver for fluid-flow, heat-transfer and combustion processes. The governing equations for dependent flow vari-

ables are presented in the general form of a differential equation. Differential equations together with mass conservation (continuity) equation are discretised by the control volume method and the resulting non-linear set of algebraic equations is solved line-by-line with a tri-diagonal matrix algorithm using the well-known pressure correction technique in a staggered calculation grid. If ϕ is a general dependent flow variable (velocity component, enthalpy, mass fraction, etc.), then the differential equation, in cartesian tensor form, for ϕ is expressed as

$$\frac{\partial}{\partial t}(\rho\phi)+\frac{\partial}{\partial x_j}(\rho u_j\phi)=\frac{\partial}{\partial x_j}\left(\Gamma_\phi\frac{\partial\phi}{\partial x_j}\right)+S_\phi \quad (1),$$

where ρ is the density of the fluid, u is velocity component, and Γ_ϕ is the exchange coefficient for variable ϕ. The source term S_ϕ depends on the solved variable. When turbulent problems are solved, the variable ϕ is the time-averaged value, and the fluctuations (Reynolds stresses, turbulent heat flux and diffusion) are expressed in terms of mean properties of the flow with the turbulence model. In most process simulations the k–ε model of turbulence is the only practical one and it is also widely used, as it is in this work.

3.2 Particle-phase equations

The Phoenics module Gentra was used for particle tracking. Built-in equations for particle position and momentum were used. The particle energy equation was, however, rewritten in order to take into account the chemical reactions. The energy equation was integrated over a small time step resulting in a particle temperature equation

$$T_p = T_g-\left(T_g-T_p^0\right)e^{-\Delta t/\tau'} +\left(\dot{q}_r A_p+\dot{Q}_s\right)\left(1-e^{-\Delta t/\tau'}\right)\Big/\pi \mathrm{Nu}\lambda_g d_p \quad (2),$$

where superscript 0 denotes the old particle temperature, $\dot{q}_r$ is the radiation heat flux between particle and gas, calculated from equation

$$\dot{q}_r = \varepsilon_p'\sigma\left(\varepsilon_g T_g^4-\alpha_g T_p^4\right) \quad (3),$$

and $\dot{Q}_s$ is the chemical reaction term calculated from equation

$$\dot{Q}_s = -\Delta H_{r,\mathrm{dis}}\left.\frac{dm_{O_2}}{dt}\right|_{\mathrm{WRL}} - \Delta H_{\mathrm{ox},p}\left.\frac{dm_{O_2}}{dt}\right|_{\mathrm{ox}} \quad (4),$$

where subscript WRL means within reacted layer, and it presents the fraction of sulphur oxidation reaction taking place inside the particle. According to Kim (Kim, 1986) this fraction can be approximated from equation

$$\left.\frac{dm_{O_2}}{dt}\right|_{\mathrm{WRL}} = \left[1-\left(\frac{d_{c1}}{d_p}\right)^3\right]\left.\frac{dm_{O_2}}{dt}\right|_{\mathrm{dis}} \quad (5).$$

Oxygen consumption terms will be discussed later in Section 4.2.

3.3 Source terms

Source terms for gas phase enthalpy and mass fraction equations are calculated after every time step. They are summed up inside one computational cell for every particle passing through that cell. The general source term equation for enthalpy due to particle-gas interaction can be written

$$\bar{S}_{h,i}^p = \sum_{n=1}^{N_p}\eta_n\dot{Q}_{i,n}\Delta t \quad (6),$$

where subscript i is for convection, radiation and chemical reaction according to equations (7)-(9), respectively.

$$\dot{Q}_c = h_{pg}\left(T_g-T_p\right)A_p \quad (7)$$

$$\dot{Q}_r = \dot{q}_r A_p \quad (8)$$

$$\dot{Q}_g = -\Delta H_{r,\mathrm{dis}}\left(\left.\frac{dm_{O_2}}{dt}\right|_{\mathrm{dis}} - \left.\frac{dm_{O_2}}{dt}\right|_{\mathrm{WRL}}\right) \quad (9)$$

Mass fraction sources are calculated simply from the sum of oxygen consumption (dm_{O_2}/dt) of each individual particle in one cell and multiplied by particle number density and the particle traverse time through that cell.

3.4 Calculation procedure

The calculation proceeds with alternating iteration of the gas flow field and solving the momentum and enthalpy equation of the particle. The procedure, known as the particle source in cell (PSIC) method, can be expressed as follows (Crowe et al., 1977):

1. Calculate the gas flow field to a more or less converged level.
2. Introduce the particles into the "frozen" flow field.
3. Calculate the particle trajectories and temperature.
4. Evaluate the particle source terms, eq. (6).
5. Solve the gas field with the sources.
6. Repeat steps 2-5 until the flow field does not change significantly.

4. KINETICS OF CHALCOPYRITE

4.1 Chemical reactions

In the mathematical model for sulphide combustion, the reactions are assumed to proceed in a similar way to that proposed by Kim (Kim, 1986). The particles to be oxidised are assumed to be initially a dense and homogeneous mixture of chalcopyrite ($CuFeS_2$) and silica (SiO_2). In the case of chalcopyrite oxidation, the overall reaction occurring can be roughly divided into three phases: thermal decomposition of the chalcopyrite particle and dissociation of the labile sulphur (10), subsequent oxidation of the diffused sulphur inside a particle and in the gas phase (11), and oxidation of the decomposed sulphide by the gas-solid (12)-(13) or gas-liquid reaction (14)-(15).

$$CuFeS_2 \rightarrow 0{,}2Cu_5FeS_4 + 0{,}8FeS + 0{,}4S \quad (10)$$

$$S + O_2 \rightarrow SO_2 \quad (11)$$

$$FeS + 1{,}67O_2 \rightarrow 0{,}33Fe_3O_4 + SO_2 \quad (12)$$

$$Cu_5FeS_4 + 0{,}5O_2 \rightarrow 2{,}5Cu_2S + FeS + 0{,}5SO_2 \quad (13)$$

$$FeS + 1{,}5O_2 \rightarrow FeO + SO_2 \quad (14)$$

$$Cu_2S + 1{,}5O_2 \rightarrow Cu_2O + SO_2 \quad (15)$$

Sulphides have a lower melting temperature than oxides, and it is assumed in the model, that a molten sulphide core, enclosed in the solid oxide crust is formed during the solid-gas reactions, and this oxide crust prevails at the outer surface of the particle during gas-liquid reactions. This is obviously a great simplification as compared to what happens in reality. The model will be enhanced in near future to take into account the experimentally observed fragmentation (Kim&Themelis, 1986; Jorgensen, 1983; Jokilaakso et al., 1991) of the particles.

4.2 Rate-controlling mechanisms

The rate controlling mechanism of oxygen consumption depends on the temperature of the particle. Below the melting point of the sulphide, gas-solid reactions prevail, and the oxygen consumption (gO_2/s) related to the thermal decomposition (10) and sulphur oxidation (11) reaction is calculated with the aid of the sulphur removal rate

$$\left.\frac{dm_{O_2}}{dt}\right|_{dis} = \pi d_p^2 \alpha \rho_p k_{di,ov} \quad (16),$$

4

where α is weight of labile sulphur per gram of sulphide.

Oxygen consumption in the particle oxidation reactions (12)-(13) is calculated from a similar kind of equation

$$\left.\frac{dm_{O_2}}{dt}\right|_{ox} = \pi d_p^2 \rho_g Y_{O_2} k_{ox,ov} \quad (17),$$

where Y_{O_2} is the mass fraction of oxygen in the gas.

The overall rate coefficients for dissociation ($k_{dis,ov}$) and oxidation ($k_{ox,ov}$) reactions are calculated from equations (18) and (19).

$$\frac{1}{k_{dis,ov}} = \frac{1}{k_d} + \frac{d_p\left(d_p - d_{c1}\right)}{2d_{c1}D_{S,eff}} + \frac{d_p^2}{d_{c1}^2 k_{dis}} \quad (18)$$

$$\frac{1}{k_{ox,ov}} = \frac{1}{k_d} + \frac{d_p\left(d_p - d_{c2}\right)}{2d_{c2}D_{O_2,eff}} + \frac{d_p^2}{d_{c2}^2 k_{ox}} \quad (19)$$

Clearly the overall rate coefficient equations include terms for external mass transfer, pore

diffusion and chemical reaction. In equation (18), d_{c1} is a diameter of an unreacted chalcopyrite core, k_d is the mass transfer coefficient, D is diffusivity, and k_{dis} is the reaction rate coefficient of the combined reactions of (10) and (11). d_{c2} is a diameter of thermally decomposed sulphide and k_{ox} is the weighted reaction rate coefficient of reactions (12) and (13). When the particle is in liquid state, the reaction rate coefficient (k_{ox}) in equation (19) is calculated from equation

$$k_{ox,l} = \sqrt{\frac{6k_d D_{O_2,l}}{d_p}} \coth \sqrt{\frac{6k_d L^2}{D_{O_2,l} d_p}} \qquad (20)$$

where $D_{O_2,l}$ is the diffusivity of oxygen in liquid, and L is the thickness of the liquid film in the film penetration concept as was proposed by Huang&Kuo (Huang&Kuo, 1963).

5. SINGLE PARTICLE OXIDATION

5.1 Role of mass transfer

The kinetic model of chalcopyrite oxidation was tested in the model of a laminar flow furnace. A large number of runs under different conditions were completed in order to distinguish the role of different mass transfer modes during particle reaction in solid and liquid states. Figures 1, 2 and 3 show the resistance of mass transfer during thermal decomposition, and particle oxidation in solid and liquid state.

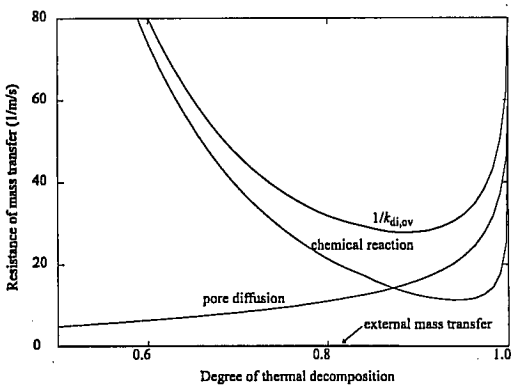

Fig 1. Resistance of mass transfer in thermal decomposition as a function of decomposition degree. T_{gas} = 873K (600°C), 21wt-% O_2, d_p = 150 μm.

Allthough most of the particles are small, the feed also consists of large particles. The case shown in Fig. 1 was calculated for a 150 μm particle. Pore diffusion is not a limiting mass transfer mode for small particles, and the thermal decomposition is controlled only by chemical reaction rate coefficient (Arrhenius equation), but for larger particles it has to be taken into account.

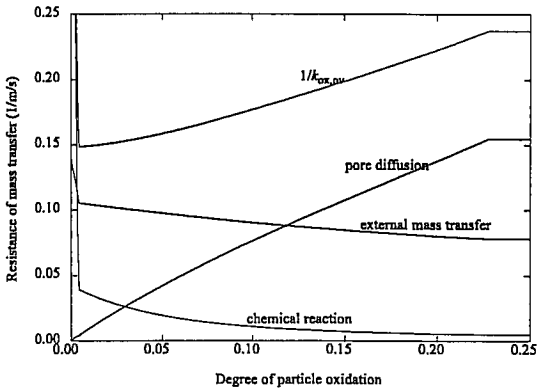

Fig 2. Resistance of mass transfer in particle oxidation in solid state as a function of reaction degree. T_{gas} = 873K (600°C), 21wt-% O_2, d_p = 50 μm.

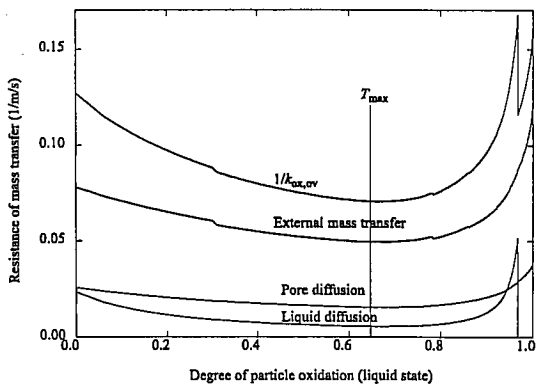

Fig 3. Resistance of mass transfer in particle oxidation in liquid state as a function of reaction degree. T_{gas} = 873K (600°C), 21wt-% O_2, d_p = 50 μm.

In Fig. 2, the particle was melted when the degree of solid state reaction reached a value of 0.23. Hence, it can be postulated that under laminar flow conditions, most of the oxidation reactions take place in the liquid state. This, however, may not be the situation in the real flash smelter where the oxygen content of the gas is totally different from that of the laminar flow furnace. Another interesting point is that pore diffusion of oxygen becomes dominant at a very early stage of reaction. In the simula-

tions, the effective diffusivity of oxygen in the reacted layer was around 7% of the bulk phase diffusion coefficient. Thus, the structure of the reaction products of oxidation reactions plays an important role in the gas-solid reaction state.

After the particle melts, the reactions are controlled mainly by external mass transfer, Fig. 3. Different values for the tortuosity of the magnetite layer were tested and a value of 4.0 was selected. However, increasing the tortuosity factor to a value 8.0 gave equal resistance of pore diffusion and external mass transfer.

Fig. 4 shows the mass fraction of minerals during particle reactions as a function of time spent in furnace, when external mass transfer controls the reactions in the liquid state. As can be seen, most of the reactions take place in a very narrow time gap (about 10 ms).

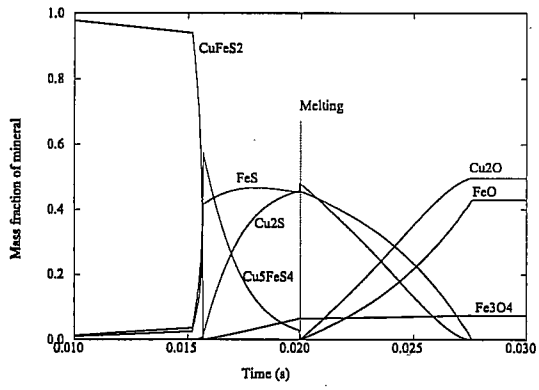

Fig 4. Mass fraction of minerals as a function of time, when external mass transfer controls the reactions in liquid state. T_{gas} = 873K (600°C), 21w-% O_2, d_p = 50 µm.

Thermally decomposed sulphides react with oxygen and practically all bornite is oxidised before the particle melts. After melting, iron and copper sulphides are assumed to react directly to oxides. This is a rough assumption, and both experimental and mathematical work is going on in order to model the gas-liquid reactions more accurately. Once again it should be kept in mind, that in a real smelter the reactions do not proceed to totally oxidised sulphides because the available oxygen is depleted to much smaller values than are present in the laminar flow furnace.

5.2 Comparison to experiments

Calculated particle temperature and sulphur removal rate were compared with published experimental data of Jorgensen (Jorgensen, 1983). Fig. 5 shows the sulphur remaining in the particle as a function of time for different gas oxygen compositions.

When compared with results published by Jorgensen, the calculated sulphur removal rates are slower for low oxygen content of gas, and higher for O_2-contents greater than 21 wt-%. Although the deviation from the measured values is obvious, the model seems to predict the influence of oxygen content correctly, e.g. with increasing oxygen enrichment the sulphur is removed more efficiently.

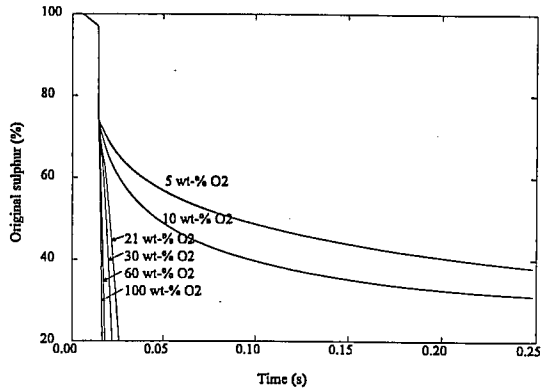

Fig 5. Percentage of original sulphur remaining in the particle as a function of time with different O_2-contents of gas. T_{gas} = 973K (700°C), d_p = 50 µm.

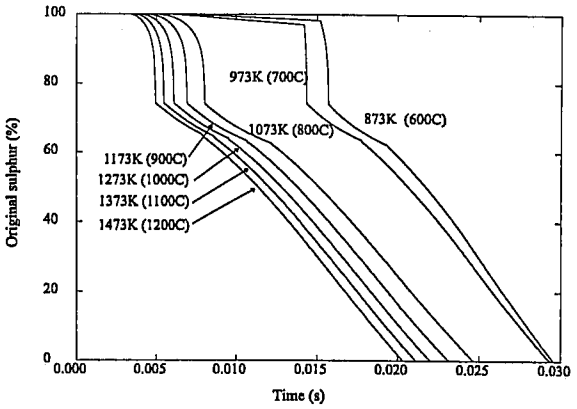

Fig 6. Percentage of original sulphur remaining in the particle as a function of time with different gas preheating temperatures. 21 wt-% O_2, d_p = 50 µm.

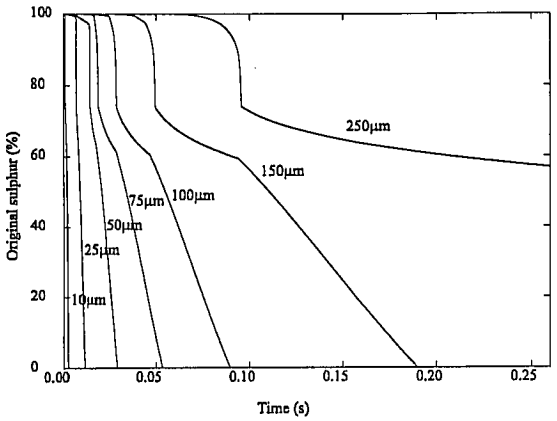

Fig 7. Percentage of original sulphur remaining in the particle as a function of time with different particle sizes. T_{gas} = 973K (700°C), 21 wt-% O_2.

In Fig 6, the sulphur content in the particle at various gas preheating temperatures is plotted against time. As compared to Jorgensen's experiments, the model over-predicts the sulphur removal at all gas preheating temperatures. However, the model predicts similar behaviour, as can be seen from Jorgensen's experiments (Appendix A).

The effect of particle size on the sulphur removal is shown in Fig. 7. For small particles up to a size of 150 μm all sulphur is removed from the particle. Larger particles only reached semimolten state and a 250 μm particle did not melt at all. Once again, the model gave a similar kind of effect on sulphur removal as was reported by Jorgensen.

6. INDUSTRIAL SIZE FURNACE

As an exemplary result of the simulations performed in an industrial size reaction shaft, Fig. 8 shows the gas phase temperatures and some particle trajectories in the upper part of the reaction shaft. Simulations were done in 2D, and a cylindrical polar coordinate system was used.

7. CONCLUSIONS

The Outokumpu flash smelting furnace is a challenging object for computer simulation due to the difference between the smallest dimensions of the distribution cone in the burner and the largest dimensions of the shaft diameter and height. Therefore, in the present modelling work, several simplifications were found necessary. However, with different models of varying grid density, the reaction shaft together with the concentrate burner could be simulated, and a lot of preliminary results were obtained concerning chalcopyrite combustion. The temperature profiles of individual particles show a similar trend to that calculated by Kim in his one-dimensional model. Also, the model predicts correctly the trend of incresing/decreasing gas preheating temperature, oxygen concentration, and particle size.

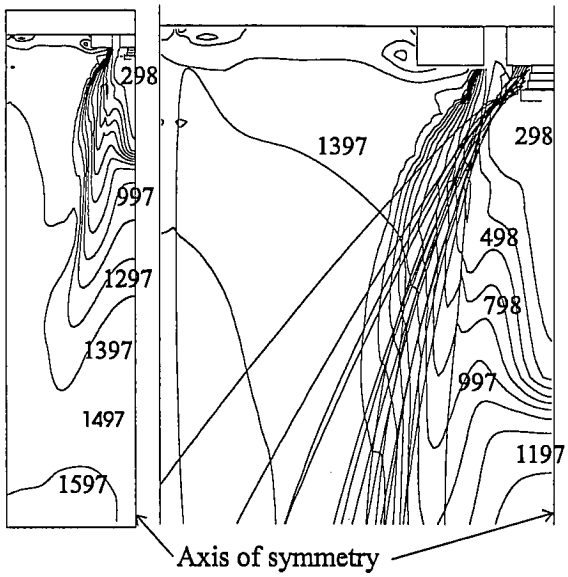

Fig. 8. Gas temperature (K) in the symmetrical slice of the reaction shaft (left) and some particle trajectories in the upper part of an industrial size flash smelting furnace reaction shaft (right).

The highly exothermic oxidation reactions and their kinetics have been coded as a separate module in the program. The model still needs a lot of further development, testing and validation, especially when the particle temperatures are high. The coupling of gas and particle phase causes also difficulties that are due to the huge amounts of heat released during the extremely fast reactions (milliseconds) after the concentrate particles ignite.

Testing and validation of the model is continuing and near future developments of the model include particle fragmentation and addition of other minerals (Cu_2S and FeS) to the model.

ACKNOWLEDGEMENTS

The authors wish to thank the Ministry of Trade and Industry, and the Technology Development Center (Tekes), Finland, and the national SULA 2 programme for financing, and Outokumpu Research Oy for permission to publish this paper. The authors are also indebted to Mr. Markku Kytö, Vice President of Outokumpu Engineering Oy, and Docent Pekka Taskinen, Pyrometallurgy Research Director of Outokumpu Research Oy, for their interest in this work and for their valuable advice.

REFERENCES

Bryk, P. et al., 1958, *Journal of Metals*, **10**, June, pp. 395-400.

Ruottu, S., 1979, The description of a mathematical model for the flash melting of Cu-concentrates, *Combustion and Flame*, **34**, pp.1-11.

Jiao, Q., Wu, L. and Themelis, N.J., 1986, "Mathematical modeling of flash converting of copper matte", J.Szekely et al., Eds., *Mathematical Modelling of Materials Processing Operations*, The Metallurgical Society, Warrendale, PA, USA, pp. 835-858.

Kim, Y., 1986, "Studies of the rate phenomena in particulate flash reaction systems: oxidation of metal sulfides", Doctoral dissertation. Columbia University.

Hahn, Y.B. and Sohn, H.Y., 1987, "Mathematical modeling of the combined turbulent transport phenomena, chemical reactions, and thermal radiation in a flash furnace shaft", J. Szekely, H. Henein and N. Jarret, Eds., *Mathematical Modeling of Materials Processing Operations*, The Metallurgical Society, Warrendale, PA, USA, pp. 799-834.

Hahn, Y.B. and Sohn, H.Y., 1990, Mathematical modeling of sulfide flash smelting process: Part I. Model development and verification with laboratory and pilot plant measurements for chalcopyrite concentrate smelting, *Met. Trans. B*, **21B**, pp. 945-958.

Smith, T.N., 1991, "Model study of gas flow in Kalgoorlie nickel smelter", *Extractive Metallurgy Conference*, pp. 245-250.

Jorgensen, F.R.A. and Elliot, B.J., 1992, "Flash Furnace Reaction Shaft Evaluation Through Simulation", *AusIMM Int. Conf. on Extractive Met. of Gold and Base Metals*, Kalgoorlie, Australia, 26-28 October, pp. 387-394.

Nguyen, T.V. et al., 1992, "Numerical Modelling of Fluid Flow, Heat Transfer and Combustion in the Kalgoorlie Nickel Smelter", *AusIMM Int. Conf. on Extractive Met. of Gold and Base Metals*, Kalgoorlie, Australia, 26-28 October, pp. 413-419.

Jorgensen, F.R.A. et al., 1995, "Modelling the burners and reaction shaft of a flash smelting furnace", Davies, T.W., Ed., *Flash reaction processes*, Kluwer Academic Publishers, Netherlands, pp. 201-238.

Jokilaakso, A. et al., 1994, "Computer simulation of fluid flow in an Outokumpu type flash smelting furnace", Sohn, H.Y., Ed., *Metallurgical Processes for the Early Twenty-First Century, Vol. I: Basic Principles*, Proceedings of the second Symposium on Metallurgical Processes for the year 2000 and Beyond, San Diego, September 21-23, pp. 841-858.

Ahokainen, T., Jokilaakso, A., 1996, "Modelling of gas-particle reactions in the copper flash smelting", *The Int. Conf. on Modelling and Simulation in Metallurgical Engineering and Materials Science*, 11 - 13 June, Beijing, China, pp.

Ahokainen, T., Jokilaakso, A., 1996, "Numerical simulation of the Outokumpu flash smelting furnace reaction shaft, Argyropoulos, A., Mucciardi, F., Eds. *International symposium on Computational Fluid Dynamics and Heat/Mass transfer Modeling in the Metallurgical Industry*, 35th Annual Conference of Metallurgists of CIM. 25.-29.8.1996, Montreal, Canada, pp. 305-319.

Kim, Y.H. and Themelis, N.J., 1986, "Effect of phase transformation and particle fragmentation on the flash reaction of complex metal sulfides", , Gaskell, D.R., Hager, J.P., Hoffmann, J.E. and Mackey, P.J., Eds., *The Reinhardt Schuhmann int. symp. on innovative technology and reactor design in extraction*

metallurgy,Warrendale, TMS-AIME, pp. 349-369.

Jorgensen, F.R.A., 1983, "Single-particle combustion of chalcopyrite", *Proc. Australas. Inst. Min. Metall.*, No. 288, December, pp. 37-46.

Jokilaakso, A. et al., 1991, Oxidation of chalcopyrite in simulated suspension smelting, *Trans. Instn. Min. Metall.* (Sect. C: Mineral Process. Extr. Metall.), **100**, May-August, C79-C90.

Huang, C-J., Kuo, C-H., 1963, General mathematical model for mass transfer accompanied by chemical reaction. *AIChE Journal*, **9**, No. 2., pp. 161-167.

Crowe, C.T., Sharma, M.P., Stock, D.E., 1977, The Particle-Source-In Cell (PSI-CELL) model for gas-droplet flows, *J. Fluids Eng.*, June, pp. 325-332.

APPENDIX A

Sulphur removal from particles as a function of time. Measurements by Jorgensen (Jorgensen, 1983).

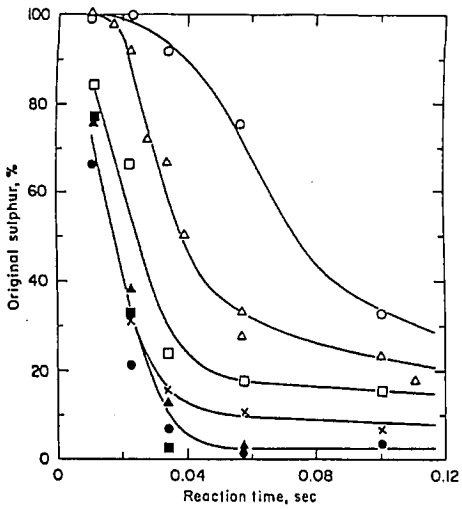

FIG. 4—The effect of experimental temperature on the combustion of 37-53 μm chalcopyrite concentrate in air. ○ 600, △ 700, □ 800, × 900, ● 1000, ▲ 1100, ■ 1200°C experimental temperatures.

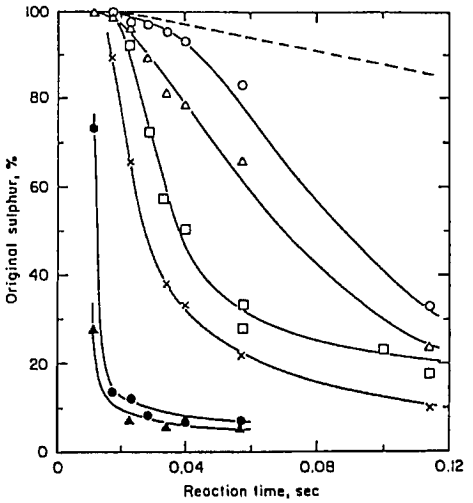

FIG. 6—The effect of oxygen concentration of the atmosphere on the combustion of chalcopyrite concentrate in oxygen-nitrogen mixtures at 700°C, 37-53 μm screen size fraction. ○ 5, △ 10, □ 21, × 30, ● 60, ▲ 100 vol.% oxygen. The dashed line is for a 1% mixture at 1000°C.

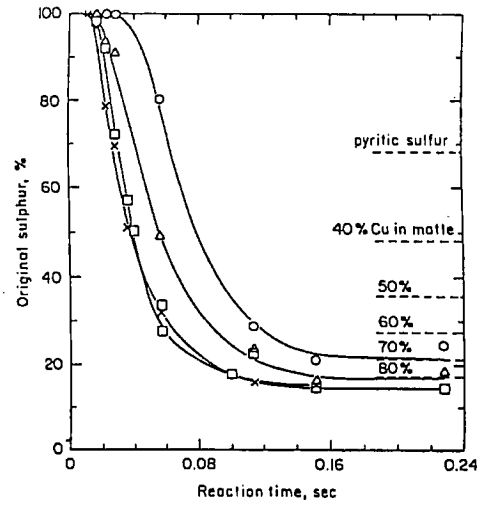

FIG. 1—The effect of concentrate sizing on the combustion of chalcopyrite concentrate in air at 700°C. ○ 74-105, △ 53-74, □ 37-53, × <37 μm screen size fractions.